The exploitation of CFD legacy for the meridional analysis and design of modern gas and steam turbines

Martina Ricci[1,*], *Roberto* Pacciani[1,**], and *Michele* Marconcini[1,***]

[1]Department of Industrial Engineering, University of Florence
Via di Santa Marta 3, 50139 Florence (Italy).

Abstract. In the last decades, the consolidation of 3D CFD approaches in the industrial design practices has progressively moved throughflow codes from the top of design systems to somewhere in between first development stages and the final aerodynamic optimizations. Despite this trend and the typical limitations of traditional throughflow methods, designers tend to still consider such methods as fundamental tools for drafting a credible aero-design in a short turnaround time. Recently a considerable attention has been devoted to CFD-based throughflow codes as suitable means to widen the range of applicability of these tools while smoothing the predictive gap with successive three-dimensional flow analyses.

The present paper retraces the development and some applications of a modern and complete CFD-based throughflow solver specifically tuned for multistage axial turbine design. The code solves the axisymmetric Euler equations with an original treatment of tangential blockage and body force. It inherits its numerical scheme from a state-of-the-art CFD solver (TRAF code) and incorporates real gas capabilities, three-dimensional flow features (e.g. secondary flows, tip leakage effects), coolant flow injections, and radial mixing models. Also geometric features of actual blades, like fillets, part-span shrouds, and snubbers, are accounted for by suitable models.

The capabilities of the code are demonstrated by discussing a significant range of test cases and industrial applications. They include single stage configurations and entire multistage modules of steam turbines, with flow conditions ranging from subsonic to supersonic. Computational strategies for design and off-design analyses will be presented and discussed. The reliability and accuracy of the method is assessed by comparing throughflow results with 3D CFD calculations and experimental data. A good agreement in terms of overall performance and spanwise distributions is achieved in both design and off-design operating conditions.

1 Introduction

Throughflow methods have been on the scene of turbomachinery design and analysis since several decades. The first throughflow codes, based on the general S1/S2 theory of Wu [1],

*Corresponding author, e-mail: martina.ricci@unifi.it
**e-mail: roberto.pacciani@unifi.it
***e-mail: michele.marconcini@unifi.it

date back to the radial equilibrium concept (Smith, [2]), the streamline curvature (Novak, [3]) or the matrix throughflow method (Marsh, [4]). Later, during the 1970s, several researcher, such as Hirsch and Warzee [5] or Denton [6], began to develop different methods for solving the governing equations of the system. There has always been a great attention in improving the capabilities of turbomachinery design methods.

Despite their relevant limitations, like the ones related to the difficulties and uncertainty in transonic and supersonic flow conditions, or to the lack of detailed resolution of the flow field inside bladed regions, throughflow methods maintained the role of workhorse tool in industrial design systems. They represented the only practical way to obtain a three-dimensional blade design, as well as applying local correlations to non uniform flows in the meridional plane.

Starting from the 1990s, with the development of computer hardware, Computational Fluid Dynamic (CFD) solvers dedicated to turbomachinery have become increasingly popular in the industrial design process. Therefore, the gradual consolidation of 3D CFD approaches has progressively moved throughflow codes from the top of design systems to somewhere in between tools typically used during the first design phases (such as one-dimensional or two-dimensional) and the three-dimensional steady and unsteady viscous solver based on CFD employed for advanced design and optimization.

Despite this trend and the typical limitations of traditional throughflow methods, designers are still relying on such methods as fundamental tools for drafting a credible aero-design in a short turnaround time.

Recently, numerical methodologies borrowed from CFD approaches have been exploited to solve the axisymmetric Euler [7] and Navier-Stokes [8] equations in the framework of time-marching throughflow solvers. This is the case of studies conducted by Gehring and Riess [9], Petrovic and Wiedermann [10, 11], Persico and Rebay [12, 13] and Simon and Léonard [14–16].

In particular, a considerable attention has been devoted to the so-called CFD-based throughflow codes as suitable means to widen the range of applicability of these tools while smoothing the predictive gap with successive three-dimensional flow analyses. In preliminary stages, they are able to provide the designer with realistic performance and spanwise distributions of flow parameters. Also, these models are able to treat any flow regime, that is subsonic, transonic or supersonic without any major issue or particular assumption, and to provide a more realistic meridional flow field with respect to classical methodologies. Shock waves occurring in bladed or unbladed regions of the flowpath can be captured without introducing specific correlations for the related losses.

The present paper retraces the development and some applications of a modern and complete CFD-based throughflow solver specifically tuned for multistage axial turbine design. The code solves the axisymmetric Euler equations with an original treatment of tangential blockage and body force, and inherits its numerical scheme from a state-of-the-art CFD solver (TRAF code, [17]). Blade body forces are calculated directly from the tangency condition to the meridional flow surface, which is iteratively adapted during the time-marching procedure to address incidence and deviation effects. Dissipative forces are computed through a realistic distribution of entropy along streamlines [18, 19]. The methodology incorporates real gas capabilities and three-dimensional flow features (like secondary flows and tip leakage effects), coolant flow injections, and radial mixing models. Also geometric features of actual blades, like fillets, part-span shrouds, and snubbers, are accounted for by suitable models [20, 21].

The capabilities of the code are demonstrated by discussing a significant range of test cases and industrial applications. They include single-stage configurations and entire multistage modules of steam turbines designed and manufactured by Ansaldo Energia, with flow conditions ranging from subsonic to supersonic. Computational strategies for design and off-

design analyses will be presented and discussed. The reliability and accuracy of the method is assessed by comparing throughflow results with 3D CFD calculations and experimental data. A good agreement in terms of overall performance and spanwise distributions is achieved in both design and off-design operating conditions.

2 Computational Framework

The system of governing equations for the throughflow analysis is based on the axysimmetric Euler equations which are written on a curvilinear coordinate system as:

$$\frac{\partial bJ^{-1}U}{\partial t}+\frac{\partial bJ^{-1}F}{\partial \xi}+\frac{\partial bJ^{-1}G}{\partial \eta}=bJ^{-1}S+J^{-1}S_b+J^{-1}S_f, \tag{1}$$

with U the conservative variables vector, F and G the inviscid flux vectors. On the right-hand side, S the source term vector arising from the formulation of the Euler equations in cylindrical coordinates, S_b the variation of tangential blockage in the blade passage and S_f the body force fields that produce flow deflection and losses.

In particular, S_f is composed by the blade body force field and the dissipative force field. The first one is intended to produce flow deflection, without generating losses. Its intensity is determined by the flow tangency condition to the streamsurface. The second one accounts for viscous losses, based on the classical distributed loss model [6]. The dissipating force is assumed to be aligned with the flow and opposite to it, so that it only results in loss generation. Its intensity is computed by empirical correlations for design and off-design conditions, and then distributed in the computational domain. Finally, an additional drag force is added to the dissipative force field to simulate the presence of part-span snubber, damping wires or snubbers, typically present in the last stages of steam turbines.

The throughflow method inherits its numerical scheme for the state-of-the-art CFD code, TRAF code. The system of governing equations is discretized with a cell-centered finite-volume scheme, and advanced in time using an explicit Runge-Kutta scheme [18]. Several numerical flux schemes are available: they range from central schemes with artificial dissipation to second order total variation diminishing (TVD) schemes built on different upwind strategies, such as the AUSM$^+$-up [21, 22].

3 Three dimensional flow features

Several novel models have been developed for three-dimensional flow effects in the throughflow framework, such as for secondary flows, tip leakage and shroud effects. The details of the models can be found in [19–21, 23], and therefore only a brief description is given here. Secondary flows have been modelled as additional 3D flow features associated with the vortices that are created when the non-uniform inlet flow is turned by the blade rows. They are accounted for via a transverse velocity field which, in a circumferentially-averaged sense, is assumed to be represented by discrete Lamb-Oseen-type vortices [19]. Tip leakage effects for shrouded and unshrouded blades are modelled in terms of source and sink convective terms [19]. The presence of part-span features, like snubbers or damping wires which are commonly encountered in steam turbine blades, is modelled in terms of an additional drag force field which is distributed locally in the area of the computational domain occupied by the cross section of the device [21].

Secondary, leakage losses are provided via correlations. They are considered on a local basis and distributed in the computational domain by suitable models. This is not sufficient to ensure a realistic representation of the spanwise distributions of flow quantities. For this

reason, in order to take into account the spanwise redistribution of flow distortions and losses, that typically occurs in multistage turbomachines, a radial mixing model has been studied and implemented [20].

4 Applications

The capabilities of the code are demonstrated by discussing a significant range of test cases and industrial applications. They include single stage configurations and entire multistage modules of steam turbines, with flow conditions ranging from subsonic to supersonic, as well as design and off-design operating conditions. The reliability and accuracy of the method is assessed by comparing throughflow results with 3D, steady, viscous, CFD calculations and experimental data.

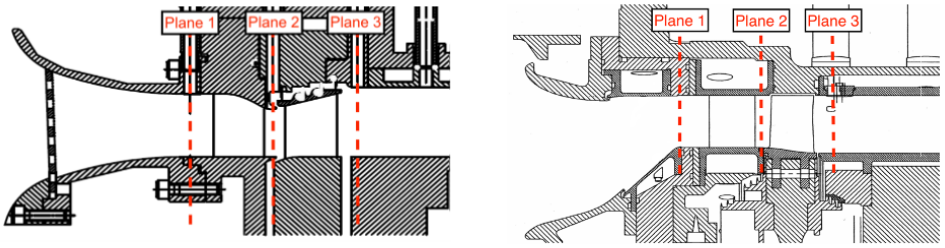

Figure 1: Meridional view of the KTH 4b stage and of the CT3 stage.

4.1 KTH 4b Stage

The first test case is a subsonic high-pressure steam turbine, the KTH 4b, an open-cycle test facility which was investigated at KTH Royal Institute of Technology [24]. The blades are mounted radially on the rotor disc while the vanes have been stacked with a certain lean angle with respect to the stator disc radial direction. The operating point investigated in the present work, which is close to the design one, has a speed of 4010 rpm, correspondig to an isentropic velocity ratio of 0.43, $\nu = (\Omega r_{mean}) / \left(\sqrt{2\Delta h_{is}} \right)$, at a fixed Reynolds number equal to $0.545 \cdot 10^6$. The facility allow us to highlight the average effect of three-dimensional flow features, especially leakage effects due to the shroud on the rotor blade.

The Ainley-Mathieson correlation [25] was used to estimate losses and the deviation angle, while for the incidence was adopted the Benner correlation [26]. Computed and measured spanwise distributions are compared in Figure 2 in terms of absolute flow angle and absolute Mach number at the outlet of each blade. A faithful reproduction is clearly evidenced for all the considered flow properties. The main discrepancies between throughflow results and measurements can be observed at the stator exit (Figures 2a, 2b), in the first 10% of the span. The relevant velocity defect together with the strong deviation are not well captured by the throughflow analysis. The effects of the shroud treatment result in a very good reproduction of the Mach number peak in the tip region (Figure 2d).

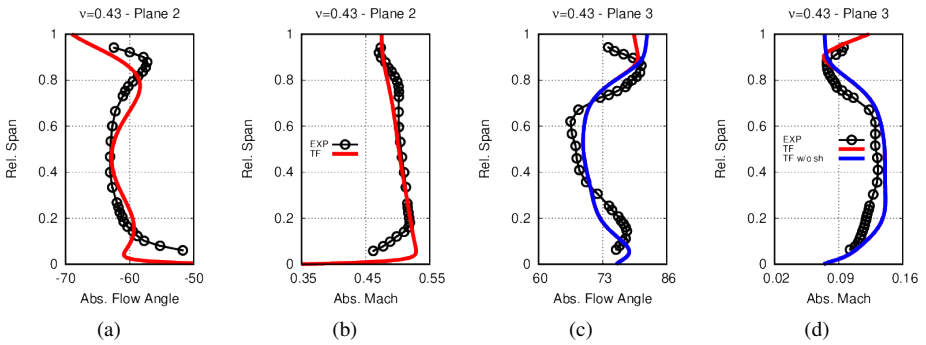

Figure 2: Predicted and measured spanwise distributions of flow quantities in planes 2 and 3 for the KTH 4b stage at $\nu = 0.43$

4.2 CT3 Stage

The second test case is a high-pressure transonic gas turbine, the CT3 stage, which was experimentally investigated at the *von Kármán Institute* [27]. The facility is able to simulate the aerodynamic performance of high-pressure turbines, reproducing the operating conditions encountered in modern aeroengine. In particular, three conditions (*Nominal*, *Low* and *High* pressure ratio) were investigated in the present work, at a fixed Reynolds number, with a rotational speed equal to 6500 rpm. The aim was to scrutinize the predictive capability of the solver at off-design conditions, and so the capability of three-dimensional flow features, without any specific calibration of the models constants.

Throughflow results are compared in terms of spanwise ditributions with experimental data and 3D, steady, viscous, CFD calculations obtained with the TRAF code [17]. At the design condition (Figures 3a, 3b, 3c, 3d) the results obtained with the throughflow solver are in very good agreement with the experimental distributions. In particular, the absolute flow angle and the total temperature (Figures 3a, 3c) are found in better agreement with respect to the 3D CFD results. Some discrepancies close to the edwalls are related to the strong distortions. The same considerations hold for the low (Figures 3e, 3f, 3g, 3h) and the high (Figures 3i, 3j, 3k, 3l) operating conditions, where we can still observe the overall good reproduction of the radial distributions of flow quantities. The particular configuration of this transonic test case, with a low aspect ratio, highlights the ability of the throughflow solver to capture the relevant changes of the radial distributions for different expansion ratios.

The predicted performance are compared with the measured values in Table 1. The calculated power is overestimated with respect to the experimental results. This slight mismatch can be connected to the appreciable discrepancies in the spanwise total pressure distributions of Figure 3b.

Table 1: Relative differences between computed operating characteristics (throughflow and 3D CFD TRAF) and measured for the CT3 stage at nominal condition.

Parameter	ε_{TF} [%]	ε_{CFD} [%]
Power	3.05	2.54

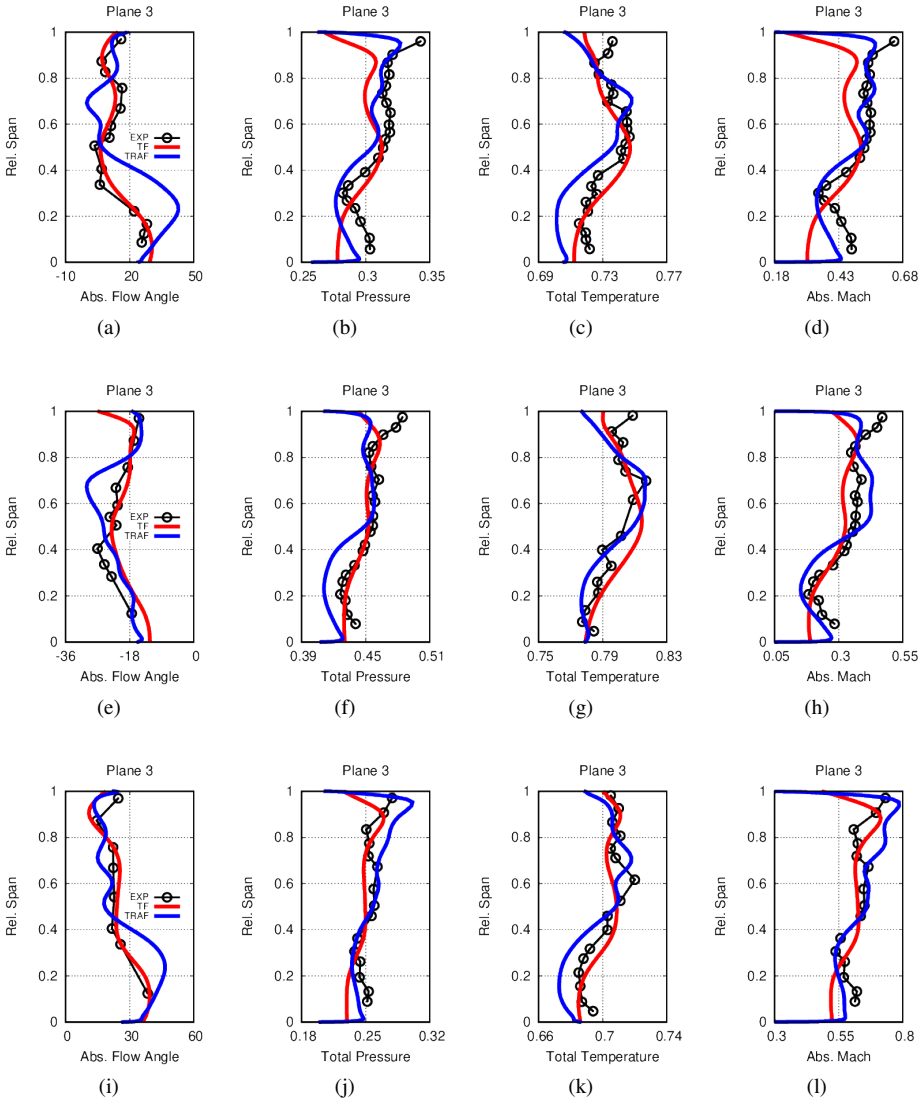

Figure 3: Predicted and measured spanwise distributions of flow quantities in plane 3 for the CT3 turbine stage at nominal (3a, 3b, 3c, 3d), low (3e, 3f, 3g, 3h) and high (3i, 3j, 3k, 3l) conditions.

4.3 Low-Pressure Steam Turbine

The capability of the procedure is further assessed by analysing the low-pressure modules of two modern large steam turbines designed and manufactured by Ansaldo Energia. These configurations are very challenging for a throughflow code: from a geometrical point of view, they share high casing flare, leaned stators and highly twisted rotors, while from an aerodynamic point of view, the last stages are characterized by very high steam velocities that convey supersonic flow at nozzle roots and rotor tips.

The first module is the the ND48 with the last rotor blade of about 48 inches high and a snubber installed at mid-span in order to overcome the structural problems. All the rotor blades are shrouded [28]. The meridional grid amounts to 76000 cells. The Craig and Cox correlation [29] was used to estimate losses, while for the deviation angle was adopted the Ainley-Mathieson correlation [25], integrated with the Traupel one for supersonic flows [30].

A first comparison between throughflow and circumferentially-averaged 3D CFD solutions in terms of the absolute Mach number is presented in Figure 4. The Mach number level predicted by the two simulations is very similar in all the three stages. A noticeable difference concerns the representation of the snubber effects. In the 3D CFD solution, the impact of the snubber is associated with a quite deep turbulent wake that spreads over a relevant span fraction as it is convected downstream. Such a behaviour cannot be reproduced in the throughflow analysis due to lack of viscous and turbulent stresses in the model. In Figure 5, the throughflow radial distributions of absolute flow angle and absolute Mach number at the last two rotors trailing edges are in satisfactory agreement with 3D CFD predictions. In particular, the distributions at the third stage outlet highlight the already noticed difference in the predicted effect of part-span snubber. Additionally, the impact of the shroud-cavity flow reinjection appears very similar in throughflow and CFD predictions, as it can be noticed in the absolute flow angle distribution near the casing at the second stage outlet.

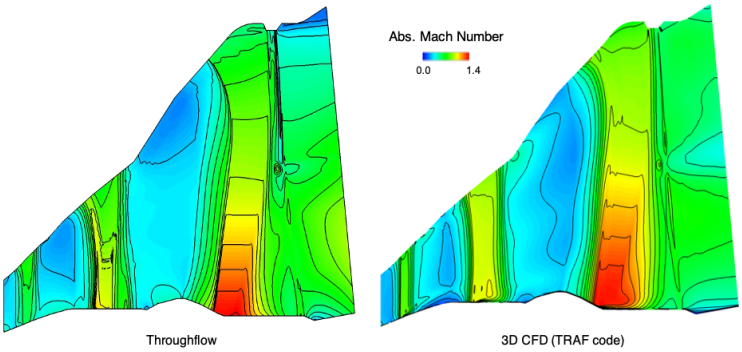

Figure 4: Computed absolute Mach number contours for the last three stage ND48 LP turbine.

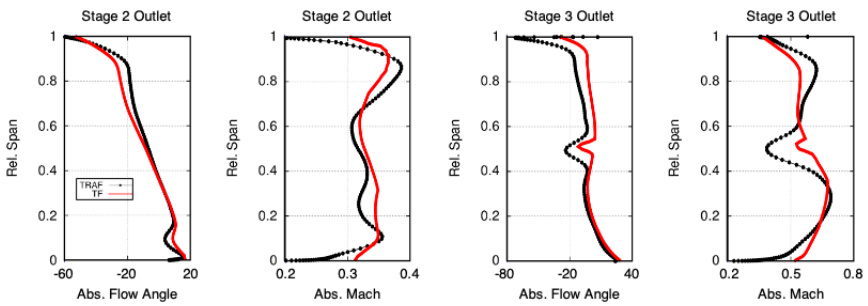

Figure 5: Spanwise distributions of flow quantities for the last two stage ND48 LP turbine.

The second low-pressure module, the Enel 320, is characterized by a pressure ratio of over 6:1, with a high peripheral speed in the last stage blade speed and a relative Mach number up to 2. A system of damping wires are presented on the last two rotor blades. Only the last rotor blade in unshrouded [31], [32].

The comparison between computed flowfields in the meridional plane is again carried out in terms of absolute Mach number contours, as shown in Figure 6. Also in this test case, the predicted levels are practically the same in all the four stages. It is important to underline the good reproduction of the peak supersonic Mach number close to the tip endwall at the last stage outlet, which is very similar to the one predicted by the 3D CFD code. Even if it is an axisymmetric shock-wave that is seldom encounterd in the actual operation of steam of gas turbines, shock capturing capabilities represent a very desirable feature in meridional analyses, as they offer an approximate but realistic way to introduce supersonic flow losses in throughflow analyses, without the need of a dedicated correlation. The accuracy achieved with the present throughflow analysis is also confirmed by spanwise distributions at the turbine exit (Figure 6), which are compared with 3D CFD results and available experimental data. The proposed tip clearance treatment is highlighted by the distributions of relative Mach number close to the casing. Instead, the effect of the damping wires can be appreciated in terms of absolute Mach number, which appears attenuated in the throughflow results with respect to 3D CFD predictions.

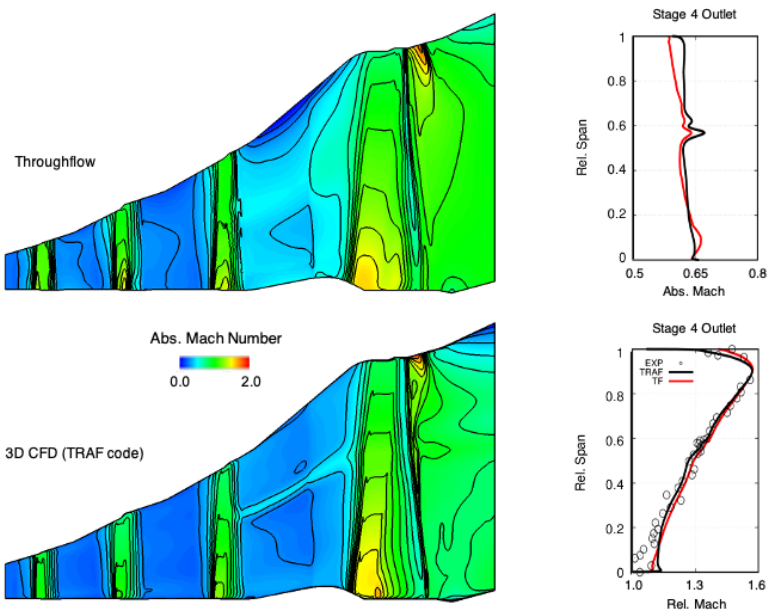

Figure 6: Computed absolute Mach number contours for the last four stage Enel 320 LP turbine, with spanwise distributions of flow quantities for the last stage.

5 Conclusion

A modern and complete CFD-based throughflow code with a widen range of applicability has been presented in this paper. Three-dimensional flow features and geometric characteristics

are accounted for by suitable models. The capabilities of the code are widely demonstrated by discussing single-stage configurations and entire multistage modules of steam turbines, with flow conditions ranging from subsonic to supersonic. The comparison between throughflow results, 3D CFD calculations, and experimental data, demonstrates the good agreement in terms of spanwise distributions and meridional flow field. It is believed that the performance of the proposed methodology is in line with the requirements of fast engineering predictions for the design of modern axial flow turbines.

Acknowledgments

The authors would thank Ansaldo Energia for the permission of publishing this paper.

References

[1] C.H. Wu, *A General Theory of Three-Dimensional Flow in Subsonic and Supersonic Turbomachines of Axial-, Radial, and Mixed-Flow Types*, Tech. rep., NACA, Report No. TN-2604 (1952)

[2] L.H. Smith, *The radial-equilibrium equation of turbomachinery*, Journal of Engineering for Power **88**, 1 (1966)

[3] R.A. Novak, *Streamline curvature computing procedures for fluid-flow problems*, Journal of Engineering for Power **89**, 478 (1967)

[4] H. Marsh, *A digital computer program for the through-flow fluid mechanics in an arbitrary turbomachine using a matrix method* (National Gas Turbine Establishment, 1966)

[5] C. Hirsch, G. Warzee, *A Finite-Element Method for Through Flow Calculations in Turbomachines*, Journal of Fluids Engineering **98**, 403 (1976)

[6] J.D. Denton, *Throughflow calculations for transonic axial flow turbines*, Journal of Engineering for Power **100**, 212 (1978)

[7] A. Sturmayr, C. Hirsch, *Throughflow model for design and analysis integrated in a three-dimensional Navier-Stokes solver*, Proceedings of the Institution of Mechanical Engineers, Part A: Journal of Power and Energy **213**, 263 (1999)

[8] Z. Yao, C. Hirsch, *Throughflow model using 3D Euler or Navier-Stokes solver*, VDI Berichte **1185**, 51 (1995)

[9] S. Gehring, W. Riess, *Analysis of the Mixing Process in a 1.5 Stage Turbine With Coolant Ejection*, Turbo Expo: Power for Land, Sea, and Air. Volume 1: Aircraft Engine; Marine; Turbomachinery; Microturbines and Small Turbomachinery (2000), v001T03A114

[10] M.V. Petrovic, A. Wiedermann, M.B. Banjac, *Development and Validation of a New Universal Through Flow Method for Axial Compressors*, Turbo Expo: Power for Land, Sea, and Air. Volume 7: Turbomachinery, Parts A and B pp. 579–588 (2009)

[11] M.V. Petrovic, A. Wiedermann, *Through-Flow Analysis of Air-Cooled Gas Turbines*, J. Turbomach. **135** (2013), 061019

[12] G. Persico, S. Rebay, *A penalty formulation for the throughflow modeling of turbomachinery*, Computers & Fluids **60**, 86 (2012)

[13] D. Pasquale, G. Persico, S. Rebay, *Optimization of Turbomachinery Flow Surfaces Applying a CFD-Based Throughflow Method*, J. Turbomach. **136** (2013), 031013

[14] J.F. Simon, O. Léonard, *A Throughflow Analysis tool based on the Navier–Stokes equations*, in *P. ETC6* (2005), pp. 7–11

[15] J.F. Simon, *Contribution to Throughflow Modelling for Axial Flow Turbomachines*, Ph.D. thesis, University of Liège (2007)

[16] J.F. Simon, J.P. Thomas, O. Léonard, *On the Role of the Deterministic and Circumferential Stresses in Throughflow Calculations*, J. Turbomach. **131** (2009), 031019

[17] A. Arnone, *Viscous analysis of three-dimensional rotor flow using a multigrid method*, J. Turbomach. **116**, 435 (1994)

[18] R. Pacciani, F. Rubechini, M. Marconcini, A. Arnone et al., *A CFD-Based Throughflow Method with An Adaptive Formulation For The S2 Streamsurface*, P. I. Mech. Eng. A-J. Pow. **230**, 16 (2016)

[19] R. Pacciani, M. Marconcini, A. Arnone, *A CFD-Based Throughflow Method with Three-Dimensional Flow Features Modelling*, International Journal of Turbomachinery, Propulsion and Power **2**, 11 (2017)

[20] M. Ricci, R. Pacciani, M. Marconcini, A. Arnone, *Secondary Flow and Radial Mixing Modelling for CFD-based Through-Flow Methods: an Axial Turbine Application*, Energy Procedia **148C**, 218 (2018)

[21] M. Ricci, R. Pacciani, M. Marconcini, P. Macelloni, S. Cecchi, C. Bettini, *Computational Fluid Dynamics-Based Throughflow Analysis of Transonic Flows in Steam Turbines*, J. Turbomach. **141** (2019), 111005

[22] M.S. Liou, *A Sequel to AUSM, Part II: AUSM$^+$-up for All Speeds*, Journal of Computational Physics **214**, 137 (2006)

[23] M. Ricci, *Improvements in CFD-based Throughflow Methods for Analysis and Design of Axial Turbines*, Ph.D. thesis, University of Florence (2020)

[24] J. Dahlqvist, J. Fridh, *Experimental investigation of turbine stage flow field and performance at varying cavity purge rates and operating speeds*, J. Turbomach. **140**, 031001 (2018)

[25] D. Ainley, G. Mathieson, *A Method of Performance Estimation for Axial-flow Turbines*, Aeronautical Research Council London (UK) **ARC R/M 2974** (1951)

[26] M.W. Benner, S.A. Sjolander, S.H. Moustapha, *An empirical prediction method for secondary losses in turbines - Part II: A new secondary loss correlation*, J. Turbomach. **128**, 281 (2006)

[27] C.H. Sieverding, T. Arts, *The VKI Compression Tube Annular Cascade Facility CT3*, Turbo Expo: Power for Land, Sea, and Air: Volume 5: Manufacturing Materials and Metallurgy; Ceramics; Structures and Dynamics; Controls, Diagnostics and Instrumentation; Education (1992), v005T16A001

[28] A. Torre, S. Cecchi, *Latest Development and Perspectives in the Optimized Design of Low Pressure Steam Turbine at Ansaldo Energia*, Proceedings of 7th European Conference on Turbomachinery Fluid dynamics and Thermodynamics (2007)

[29] H. Craig, H. Cox, *Performance Estimation of Axial Flow Turbines*, Proceedings of the Institution of Mechanical Engineers **185**, 407 (1970)

[30] W. Traupel, *Die Strahlablenkung in der vollbeaufschlagten Turbine*, Mitt. a. d. Inst. f. Therm. Turbomasch. d. ETH Zurich (1951)

[31] A. Accornero, G. Doria, L. Maretto, E. Zunino, *Flow in a 320 MW Low-Pressure Section: Theoretical and Experimental Evaluation*, Lecture series 1980-06, von Kármán Institute (1980), steam Turbines for Large Power Output

[32] A. Accornero, L. Maretto, *Aerodynamics and Streamwetness Fraction of a Multi-Stage Turbine - Comparison of Prediction with Experimental Data*, Lecture series 1983-06, von Kármán Institute (1983), aerothermodynamics of Low Pressure Steam Turbines and Condensers